Short communication

The influence of Sentinel-1 SAR sub-swath on the recorded backscatter time-series over managed hemiboreal forests

Mait Lang[1,2]* and Jaan Praks[3]

Lang, M., Praks, J. 2022. The influence of Sentinel-1 SAR sub-swath on the recorded backscatter time-series over managed hemiboreal forests. – Forestry Studies | Metsanduslikud Uurimused 77, 90–96, ISSN 1406-9954. Journal homepage: http://mi.emu.ee/forestry.studies

Abstract. The view angle range of Sentinel-1 SAR in the Interferometric Wide swath (IW) measurement mode is 29.1° – 46.0°. The dependence of backscatter on the arbitrary local incidence angle is usually corrected using a linear regression model where the incidence angle is a predictor variable. We analysed the whole time series of Sentinel-1 SAR VV-polarised backscatter over the flat 15×15 km test site in Laeva, Estonia (26° 26' 43'' E; 58° 31' 56'' N). Time series containing measurements from three different orbits were constructed for 3,159 stands from nighttime data and for 1,105 stands from daytime data. We can confirm that daytime backscatter is systematically greater than nighttime backscatter. We found a significant deviation from linearity in the backscatter dependence on local incidence angle. The empirical finding may be caused by the microwave scattering dependence on local incidence angle or by the influence of Sentinel-1 SAR sub-swath configuration in the Terrain Observation with Progressive Scans SAR (TOPSAR) method that is used for the measurements.

Key words: Sentinel-1 SAR, incidence angle, hemiboreal forest, time series, normalization.

Authors' addresses: [1]Tartu Observatory, University of Tartu, 61602 Tõravere, Tartumaa, Estonia; [2]Institute of Forestry and Engineering, Estonian University of Life Sciences, Kreutzwaldi 5, 51006 Tartu, Estonia; [3]Department of Radio Science and Engineering, Aalto University, P.O. Box 13000, 00076 Aalto, Finland; *e-mail: lang@to.ee

Introduction

The Sentinel-1 SAR is a C-band radar on sun-synchronous polar orbit (Fletcher, 2012). Sentinel-1A has been on the orbit since 3 April 2014 and Sentinel-1B since 25 April 2016, while the 1B is not functional since December 2021 due to technical problems (ESA, 2022). The radar measures microwave backscatter using the Terrain Observation with Progressive Scans SAR (TOPSAR) method by electronically steering the radar antenna over target area while the satellite is moving in azimuth direction. Measurements are done using one of four configurations. The Interferometric Wide swath (IW) mode is commonly used for land surface targets. The full ground range swath of Sentinel-1 SAR in the IW-mode is divided into three sub-swaths (Fletcher, 2012; Hajduch *et al.*, 2022).

The long Sentinel-1 SAR time series are used for prediction of soil moisture dynamics, for mapping of forests and other vegetation phenology (Van doninck *et al.*,

DOI: 10.2478/fsmu-2022-0015

© 2022 by the authors. Licensee Estonian University of Life Sciences, Tartu, Estonia. This article is an open access article distributed under the terms and conditions of the Creative Commons Attribution (CC BY) license (http://creativecommons.org/licenses/by/4.0/).

2012; Dostálová *et al*., 2018; Rüetschi *et al*., 2018). One crucial step before using SAR backscatter (σ^0) data for studies of vegetation properties is the correction or normalization of the signal for the local incidence angle (θ) that is a combination of the view angle, terrain slope and azimuth of the slope (Gauthier *et al*., 1998).

A frequently used method for normalizing SAR backscatter is to assume a linear relationship and convert the σ^0 measured at angle θ to a value at some reference angle θ_{ref}

$$\sigma^0(\theta_{ref}) = \sigma^0(\theta) - \beta(\theta - \theta_{ref}), \quad (1)$$

where β is the slope of the linear model fitted to σ^0 data using the difference $(\theta - \theta_{ref})$ as a predictor variable (Gauthier *et al*., 1998; Van doninck *et al*., 2012; Dostálová *et al*., 2018; Schaufler *et al*., 2018). The $\sigma^0(\theta_{ref})$ could be then used as a predictor variable forming dense time series for a particular target object from pixel values extracted from all overlapping image swaths viewed from different orbits.

The orbits of Sentinel-1 converge towards Earth poles and at higher latitudes it is possible to observe target objects from different orbits. In Estonia the image swaths from four to six orbits intersect on the ground. With the Sentinel-1A/1B pair on the orbit it is therefore possible during 72 hours to get three nighttime measurements and three daytime measurements for a forest stand so that an almost full-view angle range of Sentinel-1 SAR is covered in the triplets. We selected a 15 by 15 km test site near Laeva village, Estonia, in managed hemiboreal forests to study the applicability of the linear normalization (1) for the compilation of dense SAR time series.

Material and Methods

Test site

The 15×15 km test site centre coordinates are 26° 26′ 43′′ E and 58° 31′ 56′′ N. Within the area are two larger forested regions separated by river Laeva (map in Appendix 1). The topography of the area is flat. Forests in the northern bank of the river are regularly managed, but the southern region has common management history until 2019 when Raja-Kärevere nature reserve was established. Most soils in the forest land are fertile corresponding to *Aegopodium* and *Filipendula* site types (Lõhmus, 2004), however, lowland mires, transitional and raised bogs are also present. The area is influenced by long-time drainage with ditches. Dominant tree species are European aspen (*Populus tremula* L.), silver birch (*Betula pendula* Roth), Norway spruce (*Picea abies* (L.) H. Karst.), grey alder (*Alnus incana* (L.) Moench) and black alder (*Alnus glutinosa* (L.) Gaertn.). On the raised and transitional bogs dominates Scots pine (*Pinus sylvestris* L.). More details about the Laeva test site can be found in Lang *et al*. (2014). For the study we employed a database of 4,995 forest stands located in the state-owned forest land.

Sentinel-1 SAR data preprocessing

We used a stack of analysis-ready radar satellite data provided by the company KappaZeta (Kastani 42, 50410 Tartu, Estonia). The stack included interferometric coherence: 6- or 12-day repeat pass for VH and VV polarization, backscatter in VH and VV polarization mode and VH/VV backscatter ratio and local incidence angle data. Data were in raster files; pixel size 5 m. Backscatter values were computed as *sigma0* following the latest Sentinel-1 product specification (Vincent *et al*., 2020) for calibration and thermal noise correction. The terrain correction and orthorectification from radar cylindrical SLC coordinates to local L-EST 97 (EPSG:3301) coordinates was done using Copernicus 30 m resolution digital eleva-

tion model. Preprocessing details are given in Tamm *et al*. (2016).

Local incidence angle

The local incidence angle map was included in the data stack. It is based on satellite ephemeris data and Copernicus 30 m digital elevation model (DEM) (Fahrland *et al*., 2020). However, at forest edges that existed at the time of construction of the DEM occurred substantial errors that propagated into θ (Appendix 1). Within the small 15×15 km flat test site the θ varied at forest edges more than 10 degrees around its mean value. Therefore, we used constant mean incidence angle in data analysis for all stands according to relative orbits of Sentinel-1.

SAR measurement data

We used all Sentinel-1 SAR measurements that were available from the beginning of operation until the end of March 2022. From each orbit there were more than 200 images available (Table 1) for the entire study period. In this study we analysed VV polarised backscatter.

Table 1. Sentinel-1 images over Laeva test site. θ is the local incidence angle.

Tabel 1. Sentinel-1 SAR pildid Laeva testalal. θ on lokaalne langemisnurk.

Relative orbit *Orbiidi number*	*θ (deg)*	Time, UTC *Aeg, UTC*	Direction *Suund*	Images *Pilte*
058	45.5	16:00	W	254
153	31.3	04:30	E	217
160	39.3	16:00	W	281
080	38.9	04:30	E	281
087	31.7	16:00	W	233
007	45.3	04:30	E	280

Sampling of SAR backscatter from raster data

The average value of pixels found within stand border was calculated for each stand from the VV-polarized band of each image. Out of the 4,995 stands we found triple SAR measurements, i.e. sequences from three orbits for 3,159 stands at nighttime and for 1,105 stands at daytime.

Fitting of the incidence angle normalization model

We compared data from nighttime {153;080;007} and daytime {087;160;058} orbit triplets and found that daytime VV-polarized backscatter σ^0_{vv} is systematically greater than during nighttime (Figure 1). A similar note has been published by Schaufler *et al*. (2018) who found greater backscatter in the case of measurements made from ascending orbits.

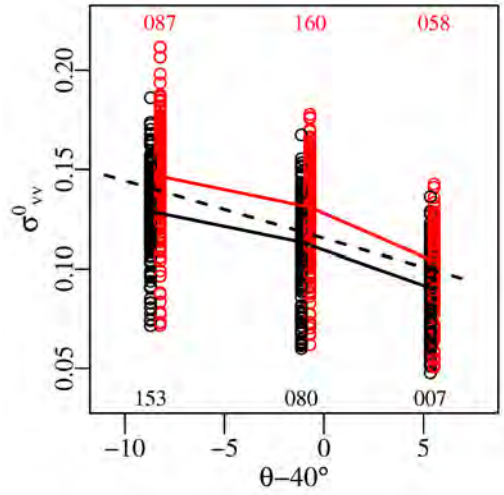


Figure 1. A mixed species stand (ID=2499). The mean value of VV-polarized backscatter σ^0_{vv} decreases more for orbit pairs 160–058 (daytime) or 080–007 (nighttime) compared to σ^0_{vv} at smaller incidence angles. Daytime σ^0_{vv} is greater compared to nighttime measurements.

Joonis 1. VV- polarisatsiooniga tagasihajumine σ^0_{vv} kahaneb rohkem orbiidipaaride 160–058 (päevane) või 080–007 (öine) korral, mille korral lokaalne langemisnurk on suurem. Päeval on tagasihajumine öisest suurem.

We separated daytime and nighttime measurements and then combined measurements according to data from orbit pairs {153–080; 080–007; 087–160; 160–058} and fitted each combination with the linear model

$$\sigma^0(\theta) = a + \beta(\theta - \theta_{ref}) + \epsilon, \qquad (2)$$

where a and β are found using least squares regression and ϵ is the model residual error.

Results and Discussion

By comparing the values of β estimated for orbit pairs we found that almost in all forest stands the mean value of σ^0_{vv} decreases more per unit angle in pairs with greater incidence angles (Figure 2). This was found in daytime as well as in nighttime measurements. If we assume that backscatter of microwave pulse follows a linear monotonous decrease through the usual SAR incidence angle range, then the application of the normalization model (1) would be justified. Based on this assumption, Van doninck *et al.* (2012) used the model (1) to normalize Advanced Synthetic Aperture Radar (ASAR) data from 80 descending passes and noted that all the observations for each image pixel were used for the model fitting. Dostálová *et al.* (2018) and Schaufler *et al.* (2018) used the model (1) for Sentinel-1 SAR data that covered large areas. In the case of Laeva Sentinel-1 SAR data set, however, (1) there is a systematic difference of backscatter from ascending and descending passes and (2) the angular correction coefficient β depends on the incident angle.

The reason for the dependence of the angular correction coefficient β on the incident angle is not clear. It is possible that forward scattering increases with θ and relatively less energy is reflected back in the case of larger local incidence angles. However, it cannot be excluded that the empirical finding is related to the Sentinel-1 SAR construction and the usage of TOPSAR measurement method. In Laeva test site the stands were located on different sub-

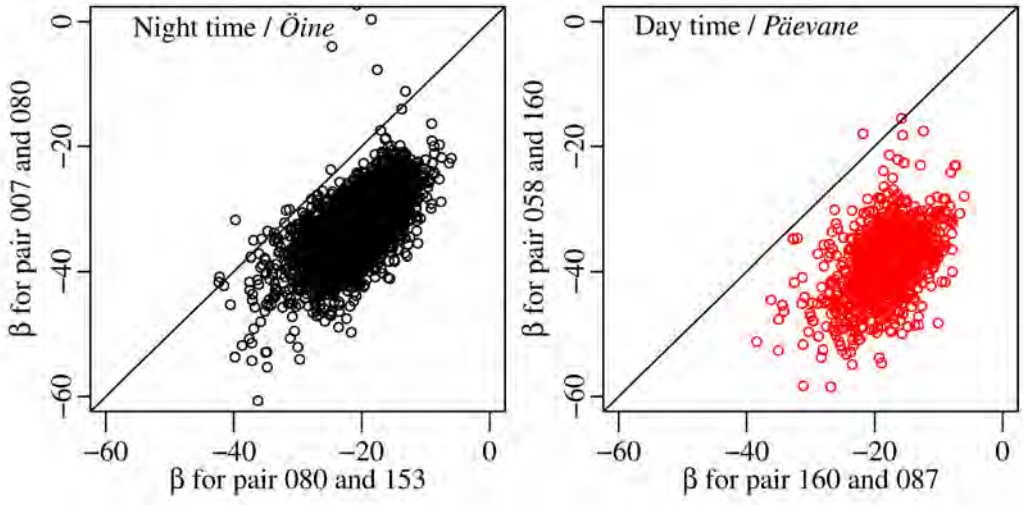


Figure 2. Slope $\beta \times 10^4$ values for model (2) fitted on VV polarized backscatter time series. Each symbol represents a single stand.

Joonis 2. Puistute aegridadele lähendatud mudeli (2) parameetri $\beta \times 10^4$ väärtused VV- polarisatsiooniga tagasihajumise korral.

swaths in the image triplets (Appendix 2). Sentinel-1 SAR calibration and signal restoration for the image construction is done by the sub-swaths (Hajduch *et al.*, 2022).

Our empirical finding may have importance for the construction of the normalized incidence angle of Sentinel-1 SAR backscatter time series for vegetation mapping and phenology studies. Fitting just a linear model on all Sentinel-1 SAR backscatter measurements over target to correct for incidence angle is not sufficient to remove the signal dependence on the influence of scanner subswath. In mapping and change detection applications the processing and decision-making accuracy may be increased if the effect of Sentinel-1 SAR subswath characteristics and the nighttime and daytime backscatter difference on the registered microwave pulse backscatter will be taken into account. Also, the 1B is not functional since December 2021 and this can create artefacts in long time series as the combination of sub-swaths over the targets is now different compared to the operational pair of Sentinel-1A and Sentinel-1B.

Acknowledgements. The data analysis was financed by the Estonian Defence Forces grant SLTTO19373. Ortophotos were made available by the Estonian Land Board. Forest inventory database material was made available by the Estonian Environmental Agency. We thank Dr Kaupo Voormansik from KappaZeta for commenting the manuscript.

References

Dostálová, A., Wagner, W., Milenković, M., Hollaus, M. 2018. Annual seasonality in Sentinel-1 signal for forest mapping and forest type classification. – International Journal of Remote Sensing, 39(21), 7738–7760. https://doi.org/10.1080/01431161.2018.1479788.

ESA. 2022. Mission Status Report 410. Reference period: 12 July 2022 – 4 August 2022. ESA Sentinel-1 Team. [WWW document]. – URL https://sentinels.copernicus.eu. [Accessed 19 August 2022].

Fahrland, E., Jacob, P., Schrader, H., Kahabka, H. 2020. Copernicus DEM, Copernicus digital elevation model. Version 2.1, Campaign ID: GEO.2018-1988-2. – Product Handbook, Taufkirchen, Germany, Airbus Defence and Space GmbH. 37 pp.

Fletcher, K. 2012. Sentinel-1: ESA's radar observatory mission for GMES operational services, ESA SP-1322/1. – ESA Report. Noordwijk, the Netherlands, ESA Communications. 85 pp.

Gauthier, Y., Bernier, M., Fortin, J.-P. 1998. Aspect and incidence angle sensitivity in ERS-1 SAR data. – International Journal of Remote Sensing, 19(10), 2001–2006. https://doi.org/10.1080/014311698215117.

Hajduch, G., Vincent, P., Cordier, K., Husson, R., Peureux, C., Schmidt, K., Piantanida, R., Recchia, A., Franceschi, N., Cotrufo, A., Mouche, A., Grouazel, A., Collard, F., Johnsen, H., Guitton, G. 2022. S-1A & S-1B Annual Performance Report for 2021. SAR-MPC-0504 - Issue 1.1 – 04/03/2022 – Project Report. CLS and MPC Consortium. 124 pp.

Lang, M., Arumäe, T., Lükk, T., Sims, A. 2014. Estimation of standing wood volume and species composition in managed nemoral multi-layer mixed forests by using nearest neighbour classifier, multispectral satellite images and airborne lidar data. – Forestry Studies / Metsanduslikud Uurimused, 61, 47–68.

Lõhmus, E. 2004. Forest site types in Estonia. (Eesti metsakasvukohatüübid). Tartu, Eesti Loodusfoto. 80 pp. (In Estonian).

Rüetschi, M., Schaepman, M.E., Small, D. 2018. Using multitemporal Sentinel-1 C-band backscatter to monitor phenology and classify deciduous and coniferous forests in northern Switzerland. – Remote Sensing, 10(1), 55. https://doi.org/10.3390/rs10010055.

Schaufler, S., Bauer-Marschallinger, B., Hochstöger, S., Wagner, W. 2018. Modelling and correcting azimuthal anisotropy in Sentinel-1 backscatter data. – Remote Sensing Letters, 9(8), 799–808. https://doi.org/10.1080/2150704X.2018.1480071.

Tamm, T., Zalite, K., Voormansik, K., Talgre, L. 2016. Relating Sentinel-1 interferometric coherence to mowing events on grasslands. – Remote Sensing, 8(10), 802. https://doi.org/10.3390/rs8100802.

Van doninck, J., Peters, J., Lievens, H., De Baets, B., Verhoest, N.E.C. 2012. Accounting for seasonality in a soil moisture change detection algorithm for ASAR Wide Swath time series. – Hydrology and Earth System Sciences, 16, 773–786. https://doi.org/10.5194/hess-16-773-2012.

Vincent, P., Bourbigot, M., Johnsen, H., Piantanida, R. 2020. Sentinel-1 product specification. Ref: S1-RS-MDA-52-7441, Issue/Revision: 3/7. – ESA Technical Document. ESA. 196 pp.

Pildi alamvälja mõju Sentinel-1 SAR mõõtmiste aegridades

Mait Lang ja Jaan Praks

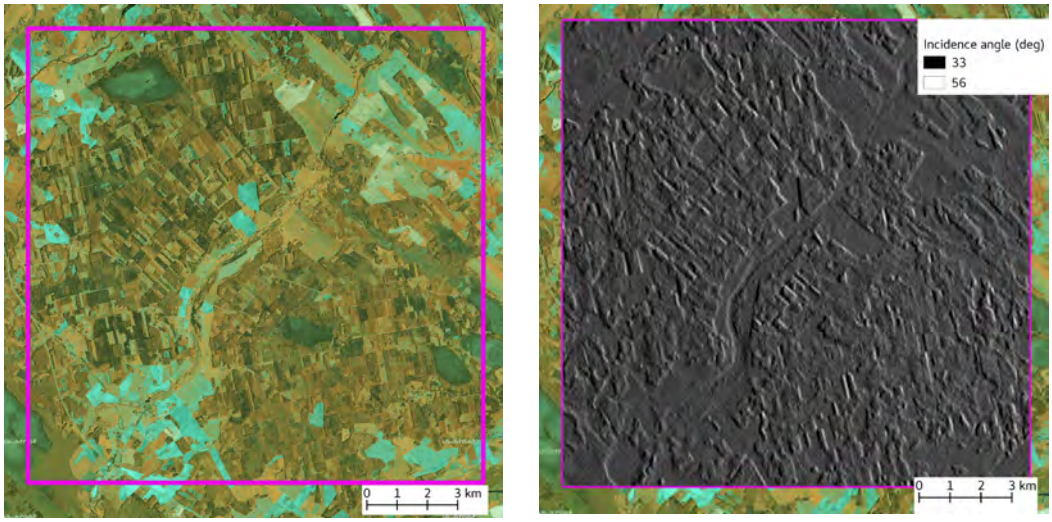
Kokkuvõte

Euroopa kosmoseprogrammi Copernicus satelliidil Sentinel-1 olev tehisavaga radar (SAR) mõõdab C-kanalis päikesesünkroonsel orbiidil (Fletcher, 2012). Sentinel-1A on orbiidil alates 3. aprillist 2014 ja Sentinel-1B alates 25. aprillist 2016, kuid 1B seiskus tehniliste probleemide tõttu 2021. aasta detsembris (ESA, 2022). Sentinel-1 SAR kasutab mõõtmiseks meetodit Terrain Observation with Progressive Scans SAR (TOPSAR). Maismaal olevaid alasid mõõdetakse Interferometric Wide swath (IW) moodis. Sentinel-1 radari vaateväli on kauguse sihis jagatud kolmeks alaväljaks (*sub-swath*) (Fletcher, 2012; Hajduch *et al.*, 2022), kui mõõdetakse IW-moodis. Radarimpulsi tagasihajumine (σ^0) sõltub lokaalsest langemisnurgast (θ), mis omakorda sõltub mõõtmisgeomeetriast (Gauthier *et al.*, 1998). Lokaalse langemisnurga mõju korrigeeritakse tavaliselt lineaarse mudeliga, teisendades nurga θ juures mõõdetud σ^0 väärtused mingi referentsnurga θ_{ref} juurde lihtsa mudeliga (1), kus β on σ^0 andmetele lähendatud lineaarseose tõus ja $(\theta - \theta_{ref})$ on mudeli argument (Gauthier *et al.*, 1998). Laeva testalal (lisa 1) selgus, et Copernicus andmebaasis olevale maapinna reljeefimudelile põhinev θ kaart on oluliselt mõjutatud metsaservadest ja seetõttu kasutasime orbiidile vastavat konstanti (tabel 1). Seejärel arvutasime igale puistule VV–polarisatsiooniga tagasihajumise keskmise iga mõõtmise kohta, valisime välja need puistud, millel oli kas päevaseid (3159 puistut) või öiseid (1105 puistut) mõõtmisi kolmelt orbiidilt ja lähendasime orbiidipaaride kaupa {153–080; 080–007; 087–160; 160–058} regressioonimudeli (2), mille tõus ongi mudeli (1) parameetriks. Selgus, et parameeter β sõltub langemisnurgast (joonised 1–2), kuigi mudel (1) eeldab sõltumatust. Empiirilise leiu põhjuseid võib olla mitu. Võimalik, et Laeva testala metsades radarimpulsi tagasihajumine kahanebki mittelineaarselt langemisnurga kasvades. Samas võib olla põhjuseks ka TOPSAR meetodis pildi alamväljade vaheline signaalitöötluse erinevus, kuna erinevatelt orbiitidelt tehtud mõõtmiste puhul satub Laeva testala pildi erinevatele alamväljadele (lisa 2). Pildi alamväljade kaupa ilmnev signaalitöötluse mõju võib tekitada vigu näiteks Sentinel-1 SAR andmete aegridadele tuginevates taimestiku fenoloogia hinnangutes, kui mõõtegeomeetria aegrea jooksul muutub näiteks koos satelliidi kaotuse või lisandumisega.

Received September 19, 2022, accepted October 03, 2022

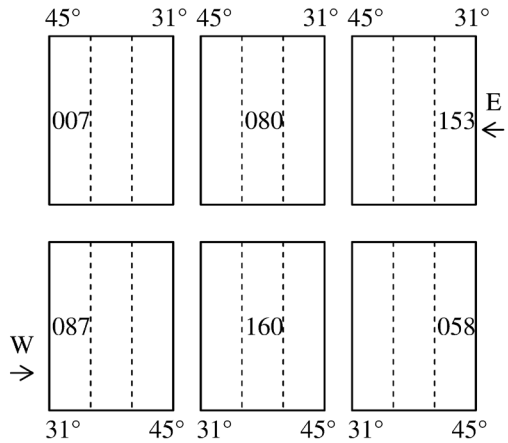
Appendix 1. False colour near infrared ortophoto (Estonian Land Board) over Laeva test site and local incidence angle map based on Copernicus DEM. Sparse vegetation is blueish, abundant herbaceous vegetation and deciduous forest are light brown, coniferous stands are dark green. Large green patches are transitional or rised *sphagnum* bogs.

Lisa 1. Testala ortofoto (Maa-amet) ja Sentinel-1 SAR lokaalse langemisnurga kaart Copernicus DEM järgi.



Appendix 2. Location of Laeva test site on Sentinel-1 SAR images taken in the Interferometric Wide swath (IW) mode is indicated by relative orbit numbers. View direction is shown with an arrow.

Lisa 2. Laeva testala asukoht Sentinel-1 SAR pildil Interferometric Wide swath (IW) moodis pildil on näidatud suhtelise orbiidi numbriga. Nool näitab vaatesuunda.



Local incidence angle / *Lokaalne langemisnurk*